

Investigation of Lattice Strain in High Energy Implanted 4H-SiC Wafers by Al or N Atoms

Zeyu Chen^{1,a*}, Hongyu Peng^{1,b}, Yafei Liu^{1,c}, Qianyu Cheng^{1,d},
Shanshan Hu^{1,e}, Balaji Raghothamachar^{1,f}, Michael Dudley^{1,g}, Reza Ghandi^{2,h},
Stacey Kennerly^{2,i} and Peter Thieberger^{3,j}

¹Department of Materials Science and Engineering, Stony Brook University, Stony Brook, 11794, NY, USA

²GE Research, Niskayuna, NY, 12309, USA

³Brookhaven National Laboratory, Upton, NY, 11973, USA

^{a*}Zeyu.chen@stonybrook.edu, ^bHongyu.peng@stonybrook.edu, ^cYafei.liu@stonybrook.edu,

^dQianyu.cheng@stonybrook.edu, ^eShanshan.hu@stonybrook.edu,

^fBalaji.Raghothamachar@stonybrook.edu, ^gMichael.dudley@stonybrook.edu, ^hghandi@ge.com,

ⁱStacey.kennerly@ge.com, ^jthieber@bnl.gov

Keywords: 4H-SiC, Ion Implantation, Lattice Strain, Synchrotron X-ray Rocking Curve Topography

Abstract. 4H-SiC wafers with 12 μm epilayer were implanted at the Tandem Van de Graaff facility at Brookhaven National Laboratory with tunable energy from 13 MeV up to 66 MeV. Lattice strains introduced by the implantation process were characterized in detail by synchrotron rocking curve X-ray topography (SXRCT) and reciprocal space maps (RSMs). It is observed that the strain levels correlate with the atomic mass and energy of acceleration of the dopant atoms.

Introduction

Silicon Carbide (SiC) is a promising semiconductor for future power devices due to its wide bandgap, high breakdown voltage and good thermal stability [1]. High voltage 4H-SiC devices are demanded for realization of hybrid aircraft and intelligent power systems. Tao Liu and coworkers have provided a theoretical model describing that deeper junction could enhance the breakdown voltage of the device [2]. Such superjunction 4H-SiC devices with thick epilayers up to 48 μm and deep junctions are therefore, being developed for high voltage (1.7 to 6.5 kV) applications. Due to the limitation of diffusion in 4H-SiC [3], multi-step ion implantation is an optimized solution for selective doping. Depth of the junction is limited to around 1 μm by conventional ion implantation since energy range to few hundred keVs is utilized [4,5]. Therefore, higher energy needs to be employed to form deep junctions. A novel multi-step high energy implantation system, allowing adjustable energy to 66 MeV, has been developed at Brookhaven National Laboratory's Tandem Van de Graaff accelerator facility [6]. Ghandi and coworkers have successfully fabricated medium voltage device with deep junction via this implantation system [7]. Ion implantation usually induces lattice strains in the SiC wafers by displacing the Si and C atoms. To comprehensively study the effect of implantation, lattice strain should be characterized in detail. C Jiang and coworkers have indicated observation of tensile strain from Xe implanted 4H-SiC by high resolution X-ray diffraction (HRXRD) [8]. Amigou and coworkers show that tensile strain also exist in N implanted 4H-SiC [9]. In this paper, extent of lattice strain of high energy Al or N implanted 4H-SiC are characterized by reciprocal space map (RSM) and synchrotron X-ray rocking curve topography (SXRCT). SXRCT has previously been successfully applied to highly sensitive strain measurement of 4H-SiC wafers [10,11,12].

Experiment

For the present experiments, two 4H-SiC wafers with 12 μm epilayer were separately implanted with Al and N atoms on two different wafers at Brookhaven National Laboratory's newly developed

multi-step high energy implantation system without annealing process. Energy ranging up to 42.99 MeV were used for N implantation, while ions with energy range of 13.8 to 65.7 MeV were employed for Al implantation. Total fluence of both implantation is $5.56 \times 10^{13} \text{ cm}^{-2}$. Sample 1 was implanted in square patterns using masks with regions between the squares unimplanted, while sample 2 was implanted with a mask covering one of the corners. The implanted samples were characterized by SXRCT at Beamline 1-BM at the Advanced Photon Source (APS), Argonne National Laboratory. A double crystal setup was used, where Si(331) beam conditioner, following the Si(111) double crystal monochromator, acts as the first crystal and 4H-SiC in (0008) reflection is the second one. The samples were rocked about the $[1\bar{1}00]$ direction in steps of 4 microradian ($0.825''$) to image the whole sample. Strain and tilt in the samples could be extracted individually by recording two series of images in 0° and 180° positions about the (0008) plane normal. Topographs were assembled by stacking the highest intensities of individual images captured by a high resolution CCD camera system with a field of view of $6.4 \text{ mm} \times 5.4 \text{ mm}$ and a pixel size of $2.5 \text{ }\mu\text{m}$. As described in previous works [10,13], strain and tilt information can be deconvoluted. 0008 RSMs were generated on a Bede D1 diffractometer with Cu $K\alpha$ ($\lambda=1.54056 \text{ }\text{\AA}$). A channel-cut Si (111) analyzer was placed in front of the detector.

Result and Discussion

Fig 1. shows 0008 reflection topographs of N implanted sample 1 and Al implanted sample 2. White contrast areas are from lead pieces used for reference purposes. The square outlines of implanted regions of sample 1 are distorted to rectangles in topograph since the diffracted beam is not exactly perpendicular to the CCD detector. Topograph from Sample 2 includes a section at the bottom right that was not implanted and therefore shows a broader contour pattern than the implanted region due to lower lattice distortion. Contours in topograph of sample 1 are broader than sample 2, indicating the extent of lattice distortion in sample 1 is lower. Within the contours, threading dislocations (TDs) are visible as white contrast dots some of which are highlighted by yellow boxes.

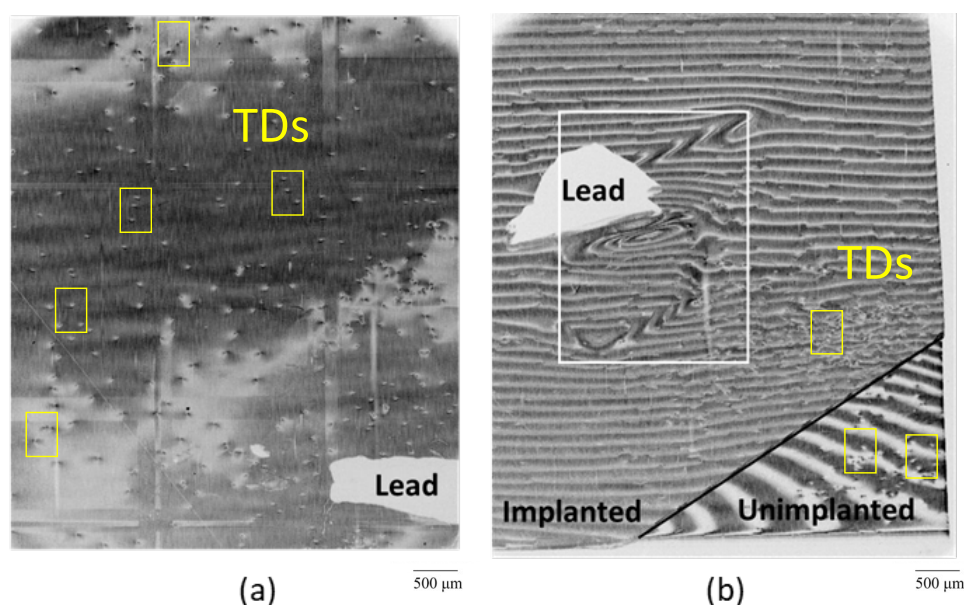


Figure 1. Topographs of (a) N implanted sample 1 (b) Al implanted sample 2 (nonuniformity of contours in white box is from the scratches)

To quantify the lattice strain, strain maps were derived from SXRCT via MATLAB using unimplanted region as reference point. Fig. 2 reveals the strain maps, RSMs of sample 1 and 2, and SRIM simulations. The strain map of sample 1 illustrates a strain level of 10^{-6} . Moreover, strain in the implanted regions is slightly tensile compared to the adjacent unimplanted regions. On the other hand, strain level of implanted region of sample 2 is 1.5 to 2.5×10^{-4} , which is almost 20 times larger

than that of sample 1. In addition, RSM of sample 1 reveals a single peak while RSM of sample 2 shows one main peak with a satellite peak lying on the bottom right. Therefore, a significant tensile strain exists in the implanted region of sample 2. The results from the strain map thus strongly correlate with the results from RSMs and reflect higher damage in sample 2 compared to sample 1.

During ion implantation, heavier dopant atoms require higher stopping energy, which is associated with displacement of Si and C atoms that results in lattice strain. Since aluminum is a heavier element than nitrogen, the damage or strain introduced by aluminum implantation is therefore larger. Damage simulations of whole energy spectrum of nitrogen and aluminum implantation via SRIM 2008 [14] has been performed. Fig. 2 (e) shows displacement per atom (dpa) versus depth profile for each implantation process. The damage is nearly uniform from surface to the planned depth of 12 μm . Overall, Al ions introduce dpa of order of 10^{-3} to the sample, which is almost 3 times higher than damage created by N ions. This difference could be attributed to difference in thickness of the Al foil that is used to increase the energy spread of the beam, energy of acceleration and atomic mass. The maximum energy of acceleration and atomic mass of Al ions are much larger than those of N ions. Besides, since the Al foil used in Al implantation is much thinner, the kinetic energy of Al ions could be larger after ions penetrated the Al foil. As a consequence, dpa created by Al implantation is more significant, which leads to a higher extent of strain in the Al implanted sample, as measured from the strain maps and RSMs.

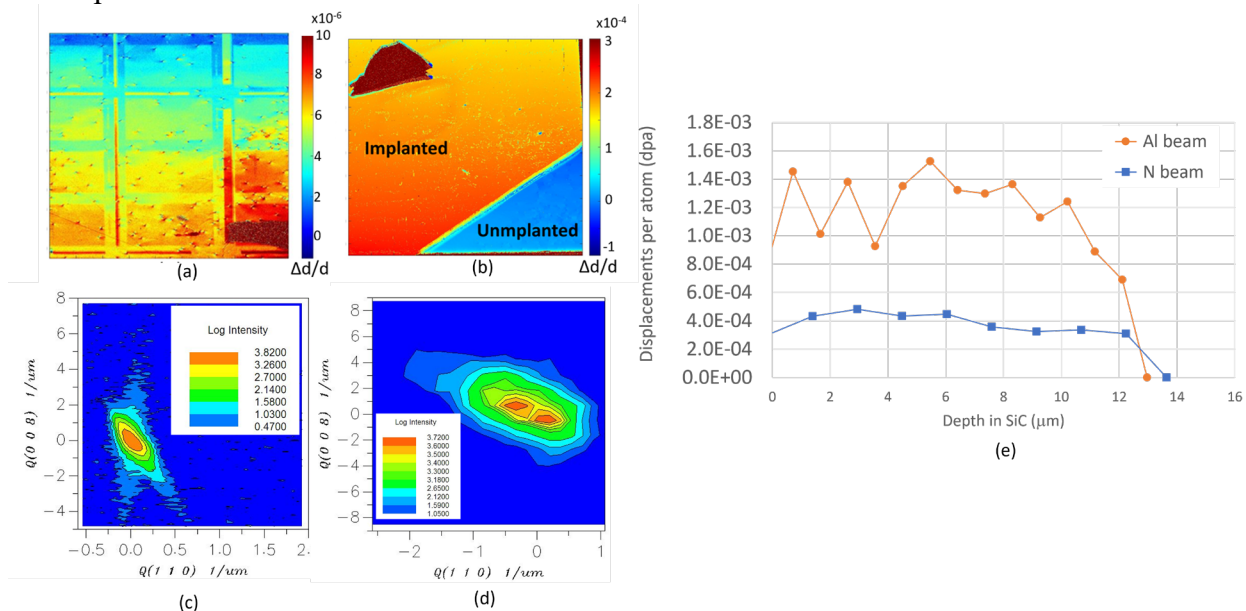


Figure 2. (a) Strain map of sample 1 (b) Strain map of sample 2 (c) RSM of implanted region of sample 1 (d) RSM of implanted region of sample 2 (e) SRIM damage simulation of sample 1 and 2 (Note: SRIM simulations account for transmission of beam through 5.75 μm Al foil (Al implantation) and 16.9 μm Al foil (N implantation) [6])

Summary

4H-SiC wafers with 12 μm epilayer, subject to high energy ion implantation by N or Al atoms at the Brookhaven National Laboratory's Tandem Van de Graaff accelerator facility, have been characterized by SXRCT and RSMs to comprehensively study the nature of lattice damage caused by implantation. Strain maps derived from SXRCT and RSMs indicate higher levels of strain in aluminum implanted wafers compared to nitrogen implanted ones. The higher atomic mass of Al and the higher maximum energy for implantation that caused higher dpa as shown by the SRIM simulations results in higher levels of strain.

Acknowledgments

Samples provided by GE Research. The information, data, or work presented herein was funded in part by the Advanced Research Projects Agency-Energy (ARPA-E), U.S. Department of Energy, under Award Number DE-AR0001028. The views and opinions of authors expressed herein do not necessarily state or reflect those of the United States Government or any agency thereof.

BNL Work supported by the U.S. Department of Energy, Office of Science, under Contract No. DE[1]SC0012704

This research used resources of the Advanced Photon Source, a U.S. Department of Energy (DOE) Office of Science User Facility operated for the DOE Office of Science by Argonne National Laboratory under Contract No. DE-AC02-06CH11357. The Joint Photon Sciences Institute at SBU provided partial support for travel and subsistence for access to Advanced Photon Source.

References

- [1] J.A.Cooper and A. Agarwal, SiC power-switching devices-the second electronics revolution? , Proceedings of IEEE, 90(6), p. 956 (2002).
- [2] T. Liu, S. Hu, J. Wang, G. Guo, J. Luo, Y. Wang, J. Guo and Y. Huo, An Investigation of Electric Field and Breakdown Voltage Models for a Deep Trench Superjunction SiC VDMOS, IEEE Access, vol. 7, pp. 145118-145123, 2019
- [3] T. Kimoto, K. Kawahara, H. Niwa, N. Kaji and J. Suda, Ion implantation technology in SiC for power device applications, 2014 International Workshop on Junction Technology (IWJT), 2014, pp. 1-6
- [4] F. Moscatelli, A. Poggi, S. Solmi and R. Nipoti, Nitrogen Implantation to Improve Electron Channel Mobility in 4H-SiC MOSFET, in IEEE Transactions on Electron Devices, vol. 55, no. 4, pp. 961-967
- [5] M. Lazar, D. Planson, K. Isoird, M. L. Locatelli, C. Raynaud and J. P. Chante, 4H-SiC bipolar power diodes realized by ion implantation, 2001 International Semiconductor Conference. CAS 2001 Proceedings (Cat. No.01TH8547), 2001, pp. 349-352 vol.2,
- [6] P. Thieberger, C. Carlson, D. Steski, R. Ghandi, A. Bolotnikov, D. Lilienfeld, P. Losee, Novel high-energy ion implantation facility using a 15 MV tandem van de graaff accelerator, Nuclear Instruments and Methods in Physics Research Section B: Beam Interactions with Materials and Atoms 442, 36-40 (2019)
- [7] R. Ghandi, A. Bolotnikov, S. Kennerly, C. Hitchcock, P.-m. Tang, T. P. Chow, 4.5 kV SiC charge-balanced MOSFETs with ultra-low on-resistance, 2020 32nd International Symposium on Power Semiconductor Devices and ICs (ISPSD), (IEEE: 2020), p 126-129
- [8] C. Jiang, A. Decl my, M. F. Beaufort, A. Boulle and J. F. Barbot, Effect of temperature on Xe implantation-induced damage in 4H-SiC, Journal of Physics: Conf. Series 1190 (2019) 012015
- [9] M. Amigou, M. F. Beaufort, A. Decl my, S. Leclerc, & J. F. Barbot, Strain Measurements on Nitrogen Implanted 4H-SiC, Materials Science Forum (2011)., 679–680, 185–188.
- [10] J. Guo, Y. Yang, B. Raghothamachar, M. Dudley, S. Stoupin, Mapping of lattice strain in 4h-sic crystals by synchrotron double-crystal x-ray topography, Journal of Electronic Materials 47, 903-909 (2018)
- [11] T. Ailiumaer, Y. Yang, J. Guo, B. Raghothamachar, M. Dudley, Studies on lattice strain variation due to nitrogen doping by synchrotron x-ray contour mapping technique in PVT-grown 4H-SiC crystals, Journal of Electronic Materials 48, 3363-3369 (2019)

-
- [12] Z. Chen, Y. Liu, H. Peng, T. Ailihumaer, Q. Cheng, S. Hu, B. Raghothamachar, M. Dudley, Characterization of 4H-SiC lattice damage after novel high energy ion implantation. ECS Transactions 104, 75 (2021)
 - [13] S. Stock, H. Chen, H. Birnbaum, The measurement of strain fields by x-ray topographic contour mapping, Philosophical Magazine A 53, 73-86 (1986)
 - [14] The Stopping and Range of Ions in Matter (SRIM) in James Ziegler's SRIM-2008 program: [http:// www.srim.org](http://www.srim.org).